

# Acinar cell ultrastructure after taurine treatment in rat acute necrotizing pancreatitis

Yuksel Ates, MD, Mehmet R. Mas, MD, Nuket Mas, PhD, Ilker Tasci, MD, Bilgin Comert, MD, Ahmet T. Isik, MD, Nuran Yener, PhD.

## ABSTRACT

**Objective:** To evaluate the organelle-based changes in acinar cells in experimental acute necrotizing pancreatitis (ANP) after taurine treatment and the association of electron microscopic findings with histopathological changes and oxidative stress markers.

**Methods:** The study was performed in February 2005 at Gulhane School of Medicine and Hecettepe University, Turkey. Forty-five rats were divided into 3 groups. Acute necrotizing pancreatitis was induced in groups II and III. Groups I and II were treated with saline and Group III with taurine 1000 mg/kg/day, i.p, for 48 hours. Histopathological and ultrastructural examinations were determined using

one-way analysis of variance and Kruskal-Wallis tests.

**Results:** Histopathologic findings improved significantly after taurine treatment. Degree of injury in rough and smooth endoplasmic reticulums, Golgi apparatus, mitochondria and nucleus of acinar cells also decreased with taurine in correlation with biochemical and histological results.

**Conclusion:** Taurine improves acinar cell organelle structure, and ultrastructural recovery in ANP reflects histological improvement.

Saudi Med J 2006; Vol. 27 (4): 446-452

Acute pancreatitis (AP) is described as a mild to severe inflammation of the gland with a clinical picture of a self-limited illness that sometimes progresses to a severe state leading to local or systemic complications including sepsis and multiple organ failure eventually causing death.<sup>1-4</sup> The exact mechanism of the disease has not been clearly identified. Accumulating data suggests a critical role for reactive oxygen species (ROS) in initiation and progression of injury.<sup>5-7</sup> Taurine (2-aminoethansulfonic acid), a free beta-amino acid derived from methionine and cysteine metabolism is normally present at high concentrations in many tissues of man and other animal species. It is involved in a number of physiological functions, including bile acid conjugation, modulation

of calcium levels and osmolarity, antioxidation, and stabilization of membranes.<sup>8</sup> Beneficial effects of taurine in decreasing tissue injury in cerulein-induced acute pancreatitis and accompanying damage in lungs through decreasing production of oxygen free radicals were shown in experimental conditions.<sup>9</sup> However, these effects were demonstrated in the early phase of the disease. Since the risk of morbidity and mortality increases as the disease progresses, new therapeutic strategies to inhibit prolongation of cellular injury in the late phase could be a new focus of interest. Histopathological changes in acute pancreatitis have been well identified. In this paper, we aimed to bring a new look to organelle based cellular changes with a higher magnification tool in experimental acute

From the Departments of Internal Medicine (Ates, Mas M, Tasci, Comert, Isik), Gulhane School of Medicine, Department of Anatomy (Mas N), Baskent University, and the Department of Anatomy (Yener) Hacettepe University, Ankara, Turkey.

Received 3rd January 2006. Accepted for publication in final form 9th March 2006.

Address correspondence and reprint request to: Dr. Ilker Tasci, Department of Internal Medicine, Gulhane School of Medicine, GATA Ic Hastaliklari BD, Etlik, 06018, Ankara, Turkey. Tel. +90 (312) 3044018. Fax. +90 (312) 3044000. E-mail: ilkertasci@yahoo.com

necrotizing pancreatitis (ANP) after treatment with a well-known potent antioxidant. We also searched for any relation between electron microscopic findings and histopathological changes or oxidative stress markers.

**Methods.** The experiments were approved by the Institutional Animal Use and Care Committee of the Gülhane Medical Academy and performed by the National Institutes of Health guidelines for the care and handling of animals.

**Animals.** Forty-five male Sprague-Dawley rats weighing 280-350 g were provided from Gülhane School of Medicine Research Center, Ankara, Turkey. The animals were housed in metabolic cages with free access to standard rat food and water at controlled temperature with 12-hour light/dark cycles for at least one week. They were fasted overnight but allowed free access to water before the experiments.

**Induction of anesthesia.** Anesthesia was induced with Sevoflurane (Sevorane® Liquid 250 ml, Abbott, Istanbul, Turkey) inhalation.

**Experiment design.** After the stabilization period, rats were randomly divided into 3 groups. All groups underwent laparotomy with manipulation and cannulation of the pancreas. Group I (Sham plus Saline, n=15) received intraductal saline injection. Groups II and III underwent induction of pancreatitis. Group II (ANP plus Saline, n=15) was injected with saline, and Group III (ANP plus Taurine, n=15) with taurine 1000 mg/kg, i.p. every 24 hours started 6 hours after the induction of pancreatitis. The animals in Group I were injected daily with saline 10 ml/kg, i.p. as controls. Fifty-four hours after the induction of pancreatitis, all surviving animals were killed with intracardiac pentobarbital (200 mg/kg) injection.

**Induction of pancreatitis.** Laparotomy was performed through a midline incision. The common biliopancreatic duct was cannulated with a 28 gauges, 0.5 inch, micro-fine catheter. Under an operating microscope, one microaneurysm clip was placed on the bile duct below the liver and another around the common biliopancreatic duct at its entry into the duodenum to avoid reflux of enteric contents into the duct. Then, 1 ml/kg of 3% sodium taurocholate (Sigma, St. Louis, MO, USA) was slowly infused into the common biliopancreatic duct and the infusion pressure was kept below 30 mm Hg, as measured with a mercury manometer.<sup>10</sup> Controls received an intraductal injection of 1 ml/kg saline. When the injection was finished, the microclips were removed, and the abdomen was closed in 2 layers. All procedures were performed using sterile techniques.

**Laboratory tests.** Blood samples for serum amylase, intraerythrocytic malondialdehyde (MDA), superoxide dismutase (SOD) and glutathione peroxidase (GSHpx) determinations were taken from the heart before killing. One portion from the pancreatic head was obtained for tissue MDA, SOD and GSHpx determinations for each animal. A Hitachi 917 autoanalyzer (Boehringer Mannheim, Mannheim, Germany) was used for the amylase assay. Erythrocyte and pancreas MDA levels were determined on erythrocyte lysate obtained after centrifugation with the method described by Jain.<sup>11</sup> After the reaction of thiobarbituric acid with MDA, the end product was measured spectrophotometrically at 532 nm. Tetrametoxo propane solution was used as standard. Malondialdehyde levels of erythrocyte was expressed as nmol/ml and pancreas as nmol/g. Erythrocyte and pancreas SOD activities were measured by a method described by Fitzgerald et al.<sup>12</sup> Briefly, the erythrocyte lysate was diluted at 400-fold with 10mM phosphate buffer, pH 7.0. In the next step, 25 $\mu$ L of diluted erythrocyte samples were mixed with 850 $\mu$ L substrate solution containing 0.05mM xanthine and 0.025mM 2-(4-iodophenyl)-3-(4-nitrophenol)-5-phenyltetrazolium chloride (INT) in a buffer solution containing 50mM CAPS and 0.94mM EDTA (pH 10.2). Then, 125  $\mu$ L xanthine oxidase (80 U/L) was added to the mixture and increases in absorbency were followed at 505 nm for 3 min against air. Various standard concentrations of phosphate buffer were used in place of a sample, as blank or standard determinations. Erythrocyte and pancreas SOD activities were expressed as U/ml and U/g. Glutathione peroxidase activities in erythrocyte lysate were measured by a previously reported method.<sup>13</sup> Briefly, 980 ml of the reaction mixture (50 mM Tris buffer, pH 7.6, containing 1 mM of Na<sub>2</sub>EDTA, 2 mM of reduced glutathione, 0.2 mM of nicotinamide adenine dinucleotide phosphate [NADPH], 4 mM of sodium azide and 1000 U of glutathione reductase) and 20 ml of erythrocyte lysate were mixed and incubated for 5 min at 37°C. Then, the reaction was initiated with 8.8 mM H<sub>2</sub>O<sub>2</sub> and the decrease in NADPH absorbency was followed at 340 nm for 3 min. Enzyme activities were reported in U/ml in erythrocyte lysate. Tissue GSHpx activity measurements were performed using a previously described method,<sup>14</sup> based mainly on the knowledge that GSHpx catalyzes the oxidation of glutathione by tertbutyl hydroperoxide. In the presence of glutathione reductase and reduced NADPH, the oxidized glutathione is immediately converted to the reduced form with concomitant oxidation of NADPH to NADP. Finally, the decrease in absorbance of NADPH at 340 nm is measured.

Glutathione peroxidase activity was expressed as U/g tissue.

**Histopathological analysis.** Tissue samples from head and tail of each pancreas were fixed in 10% neutral buffered formalin and embedded in paraffin. Paraffin sections stained with hematoxylin and eosin were examined by 2 pathologists blinded to the treatment protocol. The tissues were scored for edema, acinar necrosis, inflammatory infiltrate, hemorrhage, fat necrosis, and perivascular inflammation according to a previously described scoring system.<sup>15</sup> The scores for each histologic parameter were summed up, with a maximum score of 24.

**Ultrastructural examinations.** Other samples from the same parts were fixed in 2.5% glutaraldehyde for 24 hours, washed in phosphate buffer (pH: 7.4), post-fixed in 1% osmium tetroxide in phosphate buffer (pH: 7.4) and dehydrated in increasing concentrations of alcohol. Then, the tissues were washed with propylene oxide and embedded in epoxy-resin embedding media. Semi-thin sections about 3 mm in thickness were cut with a glass knife on a LKB (Nova ultramicrotome, Sweden). Semi-thin sections were stained with methylene blue and examined by a Nikon optiphot (Japan) light microscope. Ultra thin sections were collected on copper grids, stained with uranyl acetate and lead citrate and examined with a Jeol JEM 1200 Ex (Japan) transmission electron microscope. Thirty cells from each specimen were examined. An ultrastructural examination scoring system was defined to evaluate the results (Table 1).

**Statistical analysis.** Results were expressed as mean±SEM. The significance of differences in histopathologic scores, ultrastructural pancreatitis scores, serum amylase levels and oxidative stress markers were assessed by one-way analysis of variance and Kruskal-Wallis tests. Multiple comparisons were made by Tukey honestly significant difference (HSD) and Mann-Whitney U tests where appropriate. Correlation of histopathologic and ultrastructure scores was assessed with Pearson Correlation procedure. Probabilities less than 0.05 were considered as significant.

**Results.** Acute pancreatitis developed in Groups II and III, demonstrated by macroscopic parenchymal necrosis and abundant turbid peritoneal fluid. All animals except one in Group I, 5 in Group II, and 2 in Group III survived the experimental period of 54 hours.

**Amylase levels.** Rats in Group I had the lowest serum amylase levels, and there were statistically significant differences between the three groups (Table 2).

**Table 1 -** Ultrastructural grading system used in experimental acute pancreatitis.

Ultrastructure/assessment	Score
<b>Nucleus</b>	
Normal	0
Irregular chromatin distribution (margination, clumping)	1
Increased heterochromatin	2
Degenerated nucleus	3
<b>Mitochondria</b>	
Normal	0
Prominent cristae	1
Edematous mitochondrion	2
Collection of amorphous material	3
<b>Rough endoplasmic reticulum</b>	
Normal	0
Dilatation	1
Irregular lamellar organization	2
Presence of focal breaks	3
<b>Smooth endoplasmic reticulum</b>	
Normal	0
Dilatation	1
Vacuolization	2
Presence of large degenerated areas, myelin figures	3
<b>Golgi</b>	
Normal	0
Mild dilatation	1
Moderate dilatation	2
Severe dilatation	3

**Table 2 -** Serum amylase levels and oxidative stress markers.

Tests	Group I	Group II	Group III	P value
<b>Pancreas</b>				
MDA (nmol/g)	24.8 ± 0.8	152.1 ± 4.3	127.8 ± 3.9	0.001
SOD (U/g)	765 ± 18	248 ± 8	335 ± 12	0.001
GSHpx (U/g)	309 ± 6	83 ± 4	118 ± 4	0.001
<b>Erythrocyte</b>				
MDA (nmol/ml)	2.03 ± 0.13	9.43 ± 0.42	3.66 ± 0.21	0.001
SOD (U/ml)	784 ± 18	231 ± 8	248 ± 10	0.001
GSHpx (U/ml)	106.7 ± 3.2	18.3 ± 0.9	42.8 ± 1.8	0.001
Amylase	2076 ± 153	5428 ± 328	3872 ± 255	0.001
*one way Analysis of Variance, MDA - intraerythrocytic malondialdehyde, SOD - superoxide dismutase, GSHpx - glutathione peroxidase				

**Histological analysis.** Rats with ANP had extensive parenchymal and fat necrosis and polymorphonuclear leukocyte infiltration on histological examination. The mean  $\pm$  SEM pancreatic histology score was  $4.2 \pm 0.3$  for Group I,  $16.6 \pm 0.6$  for Group II, and  $13.9 \pm 0.6$  for Group III (**Table 3**). Histopathological scores were significantly low in Group I when compared with Groups II and III ( $p < 0.001$ , for both). Histopathological scores in Group III (ANP plus saline) were also significantly different when compared with Group II (ANP plus Taurine) ( $p < 0.002$ ). Analysis of histopathological details was given in **Table 3**. Acinar necrosis, hemorrhage and fat necrosis scores improved significantly in taurine treated group (Group III) when compared with controls (Group II) ( $p < 0.04$ ,  $p < 0.03$ , and  $p < 0.02$ ). Edema, inflammatory infiltration, and perivascular inflammation scores in Group III were also improved when compared with Group II, but the differences were not statistically significant.

**Oxidative stress markers.** Oxidative stress markers in Group I were found consistent with previous studies. In Group I, Malondialdehyde levels were lower; SOD and GSHpx levels were higher than the other 2 groups. Erythrocyte MDA levels in Group III were significantly lower than in Group II. We observed lower pancreatic MDA levels in

Group III than Group II. There was no difference in erythrocyte SOD levels between Groups III and II ( $p > 0.05$ ). Pancreatic SOD levels in Group III were significantly higher when compared to Group II. Pancreatic and erythrocyte GSHpx levels in Group III were significantly higher than Group II (**Table 2**).

**Ultrastructural analysis.** Sham plus Saline Group (Group I): Edema in acinar cells was the major finding. Interstitial edema was also observed in some samples (**Figure 1**). The ultrastructural findings in acinar cells were dilatation of rough endoplasmic reticulum and Golgi apparatus, dilatation and vacuole formation in the smooth endoplasmic reticulum, mitochondrial swelling, margination and clumping of the chromatin of the nucleus. There was no pathological finding in junctional complexes, microvilli and zymogen granules.

Acute necrotizing pancreatitis plus Saline Group (Group II): Severe edema in acinar cells and intercellular space, and myelin figures (**Figure 2a**) were observed. Dilatations and focal breaks in the rough endoplasmic reticulum; dilatations, vacuole formation and myelin figures in the smooth endoplasmic reticulum; dilatation of Golgi apparatus; edema and amorphous material collection in mitochondria (**Figure 2a**); margination and clumping of the chromatin of the nucleus (**Figure 2b**), increase

**Table 3** - Histopathologic and ultrastructural scores.

Histopathologic and ultrastructural scores	Group I	Group II	Group III	P value	
				Group I-II	Group II-III
<b>Histopathologic score</b>	$4.2 \pm 0.3$	$16.6 \pm 0.6$	$13.9 \pm 0.6$	0.001 <sup>†</sup>	0.002 <sup>†</sup>
Edema	$1.27 \pm 0.12$	$3.47 \pm 0.13$	$3.27 \pm 0.18$	0.001 <sup>‡</sup>	NS <sup>‡</sup>
Acinar necrosis	$0.33 \pm 0.13$	$2.53 \pm 0.13$	$1.93 \pm 0.18$	0.001 <sup>‡</sup>	0.033 <sup>‡</sup>
Inflammatory infiltration	$0.93 \pm 0.06$	$2.67 \pm 0.13$	$2.47 \pm 0.13$	0.001 <sup>‡</sup>	NS <sup>‡</sup>
Hemorrhage	$0.93 \pm 0.07$	$2.87 \pm 0.09$	$2.33 \pm 0.16$	0.001 <sup>‡</sup>	0.026 <sup>‡</sup>
Fat necrosis	$0.33 \pm 0.13$	$2.53 \pm 0.17$	$2.00 \pm 0.10$	0.001 <sup>‡</sup>	0.0192 <sup>‡</sup>
Perivascular inflammation	$0.33 \pm 0.13$	$2.53 \pm 0.13$	$2.13 \pm 0.17$	0.001 <sup>‡</sup>	NS <sup>‡</sup>
<b>Ultrastructural score</b>	$137 \pm 3$	$252 \pm 5$	$158 \pm 3$	0.001 <sup>†</sup>	0.001 <sup>†</sup>
Nucleus	$22.6 \pm 0.5$	$34.9 \pm 1.3$	$24.5 \pm 0.4$	NS <sup>†</sup>	0.001
Mitochondria	$34.4 \pm 0.9$	$50.8 \pm 1.4$	$42.5 \pm 1.1$	0.001	0.001 <sup>†</sup>
RER	$24.6 \pm 0.9$	$61.1 \pm 1.4$	$29.3 \pm 0.9$	0.001 <sup>†</sup>	0.001 <sup>†</sup>
SER	$27.3 \pm 0.7$	$62.2 \pm 1.4$	$32.7 \pm 1.1$	0.004 <sup>†</sup>	0.001 <sup>†</sup>
Golgi	$27.7 \pm 0.7$	$43.2 \pm 1.9$	$29.1 \pm 0.7$	NS <sup>†</sup>	0.001 <sup>†</sup>

<sup>†</sup>Turkey honestly significant difference; <sup>‡</sup>Mann-Whitney U test, NS = not significant, RER - Rough endoplasmic reticulum, SER - smooth endoplasmic reticulum



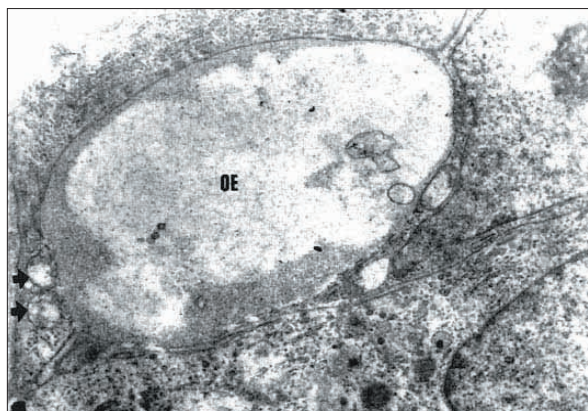


**Figure 1** - Electron micrograph showing intercellular edema (OE) and swollen mitochondria (arrows) in the sham group. (Original magnification x 6000).

in heterochromatin were observed on ultrastructural examination of the pancreatic acinar cells. Microvilli and zymogen granules were found normal. The severity of ultrastructural changes in this group was more severe than the other groups. Edema in intercellular junctions was also observed.

Acute necrotizing pancreatitis plus taurine group (Group III): Intracellular and intercellular edema were observed in all specimens (**Figure 3a**). Although the degree of intracellular edema was similar, edema in intercellular junctions was more severe than Group I. Another finding was the presence of myelin figures in pancreatic acinar cells (**Figure 3b**). Dilatation of the rough endoplasmic reticulum and Golgi apparatus, dilatation and vacuole formation in the smooth endoplasmic reticulum, mitochondrial swelling, margination and clumping of the chromatin of the nuclei were the other ultrastructural findings (**Figures**

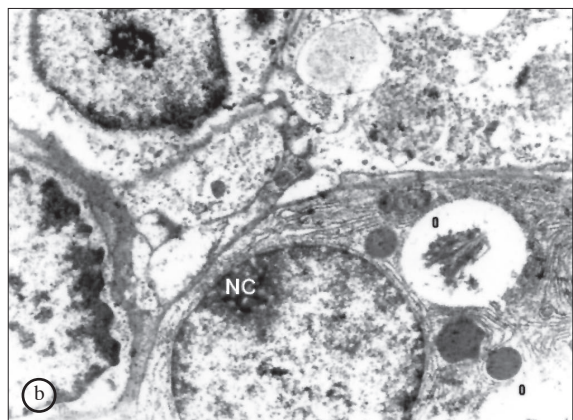
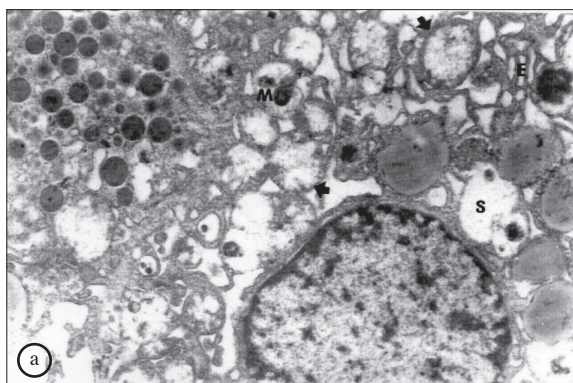


**Figure 2** - Electron micrograph showing **a**) myelin figures (M), swollen mitochondria (arrows), dilated RER (E) and dilated SER (S) in Group II. (Original magnification x6000) and **b**) the intracellular edema (O), margination and clumping of the chromatin of the nucleus (NC) in Group II. (Original magnification x 6000)

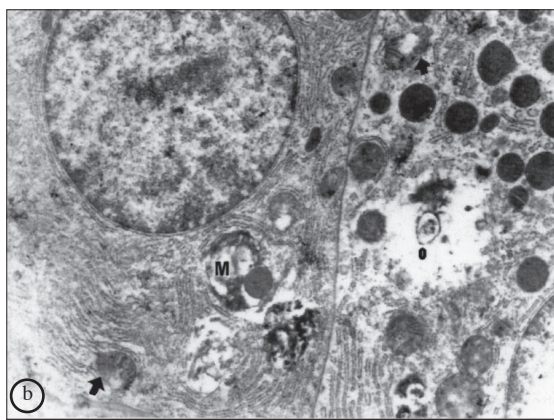
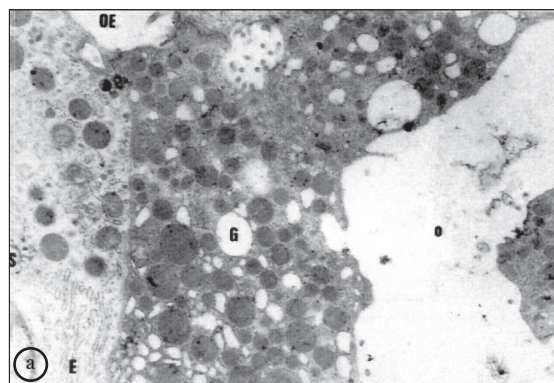


**Figure 3** - Electron micrograph showing **a**) the intracellular edema (O), intercellular edema (OE), dilated RER (E), dilated SER (S), dilated Golgi apparatus (G) in Group III. (Original magnification x6000) and **b**) the myelin figures (M), swollen mitochondria (arrows) and intracellular edema (O) in Group III. (Original magnification x 6000).

**3a & 3b).** No pathological finding was observed in the microvilli and zymogen granules.

Ultrastructural scores in all 3 groups highly correlated with histopathological scores ( $r = 0.897$  for Group I,  $r = 0.918$  for Group II, and  $r = 0.913$  for Group III).

**Discussion.** Approximately 20-30% of all patients with acute pancreatitis develop a severe clinical course during the initial 24-48 hours after the onset of symptoms.<sup>15</sup> Organ dysfunction and pancreatic/peripancreatic necrosis is initiated by 'premature' intra-acinar activation of digestive enzymes which trigger a systemic inflammatory response. The role of oxidative stress has been extensively evaluated in different experimental models of acute pancreatitis. Generation of ROS and accumulation of lipid peroxidation products with concomitant depletion anti-oxidants in pancreas are all involved in pathogenesis of cerulein induced acute pancreatitis.<sup>16</sup> Taurine supplementation has been reported to improve histopathological findings and oxidative stress markers in a rodent model of ANP.<sup>17</sup> Antioxidant effects of taurine can be reached when administered around one g/kg/day in such models.<sup>17,18</sup> Our results confirm the previous reports that, at a biologically acceptable dose, taurine diminishes the degree of histopathological injury and oxidative stress. However, we mainly focused on the ultrastructural changes in the nucleus, rough endoplasmic reticulum, smooth endoplasmic reticulum, Golgi apparatus, and mitochondria after treatment with taurine in the present study. Understanding the nature of ultrastructural changes in ANP requires detailed examination of acinar cells that constitute the major site of injury, the acini. Under transmission electron microscope, we observed neither organelle was wholly preserved nor damaged during the injurious course; instead, a generalized derangement was visible for every organelle. This led us to design a scoring system on the basis of specific findings for each organelle which can be ascribed to the degree of ultrastructural injury for the whole acinar cell. Hopefully, this would bring us the advantage of getting more precise and standard data about the injury and level of healing with or without taurine treatment. Although we noted marked intracellular/intercellular edema in established pancreatitis, we left it outside the range of scoring table since we aimed to measure the degree of injury only for the "organelles". We also did not consider cell membrane since we have chosen the cells with intact membranes. Because sodium taurocholate most probably causes acute pancreatitis by cleaving the cell membranes through the detergent effects of

bile salts,<sup>19,20</sup> excluding the degree of cell membrane injury may be a drawback of this method. When we assessed our results according to this scoring table, we noticed that all the acinar cell organelle scores in taurine treated rats were significantly improved when compared with controls. Furthermore, nucleus and Golgi scores in specimens from taurine treated animals were statistically not different from sham operated animals, suggesting that recovery is fastest and complete reversibility of structural damage can be considered for these 2 organelles (Table 3). We injected sodium taurocholate into the main pancreatic duct system below natural secretory pressure in order to preserve microvilli on the apical portions and not to cause rupture and release of bile salts into the interstitium. Indeed, the microvilli on the apical portions of injured acinar cells were well preserved in our samples. Therefore, it is likely that sodium taurocholate diffuses through the interstitium around the acini without reaching the acinar lumen as it was proposed previously.<sup>20</sup> Zymogen granules, acinar cell specific elements in the cytoplasm, were carefully examined. Number and distribution of the zymogen granules were similar in both treated and untreated pancreatitis groups. Normally, these granules are resistant to toxic effects of bile salts;<sup>21</sup> thus, preservation of normal localization, structure and number of zymogen granules after sodium taurocholate injection could not be an exclusive finding. An interesting point of this study was that, after taurine treatment, the ultrastructural improvements were more remarkable than histopathological recovery according to scoring system. This might have occurred not only due to scary characteristics of tissue healing in the pancreas but also to the fact that recovery starts primarily within the acinar cells. Less comparable results are likely to be obtained if taurine treatment is prolonged to a time enough for broad tissue healing. We have previously described the ultrastructural changes after taurine administration during the early course of ANP (unpublished data). In the present work, we further analyzed the effects of taurine at 48th hour time point, which represents a relatively late stage of the disease. There were not many differences in the degree of ultrastructural findings with prolonged taurine treatment, suggesting that organelle recovery is completed in the early phase if the injurious cascade is blocked. However, tissues from taurine treated animals had much less inflammatory infiltration and fibrosis, the latter being a common feature of chronic pancreatitis. It is a predictable point that acinar cell recovery is followed by decrease in inflammation and subsequent fibrosis. On the other hand, ultrastructural view of this study does not cover evaluation of infiltration or fibrosis. Organelle injury scores also



correlated well with markers of oxidative stress, which was shown to be involved in the pathophysiological events in the late phase.<sup>22</sup>

In conclusion, ultrastructural recovery in the acinar cells starts earlier than histopathological improvements in ANP. Efforts to develop injury determination methods namely a scoring system including the findings in major organelles, other structures, and pathologies can help reaching more valid results.

**Acknowledgment.** This work was supported by grants from the Gülhane Medical Research Council (Project no: AR-01/01) and Department of Anatomy, Hacettepe University, Ankara, Turkey.

## References

1. Braganza JM. Experimental acute pancreatitis. *Curr Opin Gastroenterol* 1990; 6: 763-768.
2. Grendell JH. Acute pancreatitis. *Curr Opin Gastroenterol* 1995; 11: 402-406.
3. Steer ML. Pathogenesis of acute pancreatitis. *Digestion* 1997; 58: 46-49.
4. Lerch MM, Adler G. Experimental animal models of acute pancreatitis. *Int J Pancreatol* 1994; 15: 159-170.
5. Sweiry JH, Mann GE. Role of oxidative stress in the pathogenesis of acute pancreatitis. *Scand J Gastroenterol* 1996; 219: 10-15.
6. Schoenberg MH, Buchler M, Beger HG. Oxygen radicals in experimental acute pancreatitis. *Hepatogastroenterology* 1994; 41: 313-319.
7. Schoenberg MH, Birk D, Beger HG. Oxidative stress in acute and chronic pancreatitis. *Am J Clin Nutr* 1995; 62: 1306S-1314S.
8. Huxtable RJ. Physiological actions of taurine. *Physiol. Rev* 1992; 72: 101-163.
9. Ahn BO, Kim KH, Lee G, Lee HS, Kim CD, Kim YS. Effects of taurine on cerulein-induced acute pancreatitis in the rat. *Pharmacology* 2001; 63: 1-7.
10. Liu Q, Djuricin G, Rossi H, Bewsey K, Nathan C, Gattuso P, et al. The effect of lexipafant on bacterial translocation in acute necrotizing pancreatitis in rats. *Am Surg* 1999; 65: 611-616.
11. Jain SK. Hyperglycemia can cause membrane lipid peroxidation and osmotic fragility in human red blood cells. *J Biol Chem* 1989; 264: 21340-21345.
12. Fitzgerald SP, Campbell JJ, Lamont JV. The establishment of reference ranges for selenium. The selenoenzyme glutathione peroxidase and the metalloenzyme superoxide dismutase in blood fractions. The 5th International Symposium on *Selenium Biology and Medicine* 1992; Tennessee: 20-23.
13. Pleban PA, Munyani A, Beachum J. Determination of selenium concentration and glutathione peroxidase activity in plasma and erythrocytes. *Clin Chem* 1982; 28: 311-316.
14. Paglia DE, Valentine WN. Studies on the quantitative and qualitative characterization of erythrocyte glutathione peroxidase. *J Lab Clin Med* 1967; 70: 158-169.
15. Schmidt J, Rattner DW, Lewandrowski K, Compton CC, Mandavilli U, Knoefel WT, et al. A better model of acute pancreatitis for evaluating therapy. *Ann Surg* 1992; 215: 44-56.
16. Buchler MW, Uhl W, Friess H, Malfertheiner P, editors. Acute Pancreatitis-Novel Concepts in Biology and Therapy. Berlin: Blackwell Publishers; 1999. p. 77-87.
17. Ozturk M, Mas MR, Yasar M, Ozturk M, Mas MR, Yasar M, et al. The role of inducible nitric oxide synthase inhibitor, meropenem, and taurine in experimental acute necrotizing pancreatitis. *Pancreas* 2003; 26: 357-362.
18. Gurer H, Ozgunes H, Saygin E, Ercal N. Antioxidant effect of taurine against lead-induced oxidative stress. *Arch Environ Contam Toxicol* 2001; 41: 397-402.
19. Helenius A, Simons K. Solubilization of membranes by detergents. *Biochim Biophys Acta* 1975; 415: 29-79.
20. Aho HJ, Nevalainen TJ. Experimental pancreatitis in the rat. Ultrastructure of sodium taurocholate induced pancreatic lesions. *Scand J Gastroenterol* 1980; 15: 417-424.
21. Backwinkel KP, Schriewer H, Rauen HM, Themann H. Ultrastrukturelle aspekte zur pathogenese der deoxycholatlpankreatitis. *Res Exp Med* 1975; 166: 43-52.
22. Yasar M, Mas MR, Comert B, Akay C, Deveci S, Yilmaz MI, et al. Has the Oxidative Stress a Role in Late Phase of Experimental Acute Necrotizing Pancreatitis? *Hepatogastroenterology* 2002; 49: 1692-1695.